The Journal of Chemical Physics

RAPID COMMUNICATION | FEBRUARY 23 2026

Configurational entropy of randomly double-folding ring polymers

Pieter H. W. van der Hoek ; Angelo Rosa ; Elham Ghobadpour ; Ralf Everaers

J. Chem. Phys. 164, 081101 (2026)
https://doi.org/10.1063/5.0318212

The Journal of Chemical Physics COMMUNICATION pubs.aip.org/aip/jcp

Configurational entropy of randomly double-folding ring polymers

Cite as: J. Chem. Phys. 164, 081101 (2026); doi: 10.1063/5.0318212
Submitted: 19 December 2025 • Accepted: 6 February 2026 •
Published Online: 23 February 2026

Pieter H. W. van der Hoek,[1,a] Angelo Rosa,[1,b] Elham Ghobadpour,[2,c] and Ralf Everaers[2,d]

AFFILIATIONS

[1] SISSA - Scuola Internazionale Superiore di Studi Avanzati, Via Bonomea 265, 34136 Trieste, Italy
[2] ENS de Lyon, CNRS, Laboratoire de Physique (LPENSL UMR5672) et Centre Blaise Pascal, 69342 Lyon cedex 07, France

[a] **Electronic mail:** pvanderh@sissa.it
[b] **Author to whom correspondence should be addressed:** anrosa@sissa.it
[c] **Electronic mail:** elham.ghobadpour@ens-lyon.fr
[d] **Electronic mail:** ralf.everaers@ens-lyon.fr

ABSTRACT

Topologically constrained genome-like polymers often double-fold into tree-like configurations. Here, we calculate the exact number of tightly double-folded configurations available to a ring polymer in ideal conditions. For this purpose, we introduce a scheme that allows us to define a "code" specifying how a ring wraps a randomly branching tree and calculate the number of admissible wrapping codes via a variant of Bertrand's ballot theorem. As a validation, we demonstrate that data from Monte Carlo simulations of an elastic lattice model of non-interacting tightly double-folded rings with controlled branching activity are in excellent agreement with exact expressions for branch-node and tree size statistics that can be derived from our expression for the ring entropy.

INTRODUCTION

Topologically constrained genome-like polymers often double-fold into tree-like configurations as they form plectonemes due to supercoiling,[1–4] undergo loop extrusion,[5–9] or maximize the entropy of the crumpled[10] territorial[11] arrangement of interphase chromosomes arising from the decondensation of topologically untangled metaphase chromosomes.[12–14] Randomly branching double-folded ring polymers were first discussed theoretically[15–19] and then explored numerically[20–25] in the context of dense solutions and melts of unknotted and non-concatenated ring polymers.[26] Figure 1(a) schematizes the progression from an off-lattice representation of a double-folded ring, over the association of a randomly branching tree characterizing the secondary structure,[27] to a lattice model[17,28,29] of tightly double-folded rings with reptons[30] representing stored length. The purpose of the present work is to calculate the configurational entropy of randomly double-folded rings in ideal conditions. To this end, we introduce a scheme that allows us to define a "code" specifying how a ring wraps a randomly branching tree, calculate the number of admissible wrapping codes, and present a detailed comparison of theoretical predictions and corresponding simulation data for a variant of the elastic lattice model introduced in Refs. 28 and 29, which allows us to control the branching activity.

NON-INTERACTING TREES CHARACTERIZING DOUBLE-FOLDING IN THE ABSENCE OF VOLUME INTERACTIONS

In analogy to the standard phantom chain model,[31,32] the present work focuses on double-folding in the absence of volume interactions. While their inclusion in simulations is straightforward[33–36] and their effects can be rationalized by Flory theory,[18,37,38] exact treatments remain a challenge.[39–42] Below, we distinguish between *configurations* and *conformations* following the standard notation in the fields of graph theory and polymer physics. In particular, we use the term *configuration* to refer to the connectivity of a tree or the secondary structure[27] of a double-folded ring, while we employ *conformation* to designate a spatial embedding [Fig. 1(b)]. Specifically, we consider double-folding onto *acyclic*

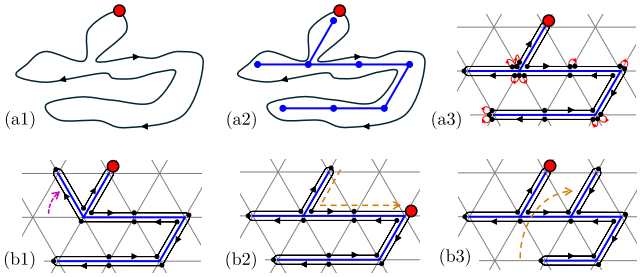

FIG. 1. Illustration of the modeling steps and notation used in this work. In various physical and biological situations, (ring) polymers double-fold into conformations (a1) that can be characterized via acyclic trees (a2) and represented by (elastic) lattice models (a3) along the lines of Refs. 17, 28, and 29 where we have highlighted the monomer labeled "1" in red. (b1) Another *conformation* of the embedded ring for the same *configuration* of the tree and the same secondary structure of the double-folded ring. (b2) A cyclic permutation of the ring around the tree corresponds to a different *configuration* or secondary structure of the ring. (b3) A different tree *configuration* and hence also a different *configuration* of the double-folded ring.

trees embedded on a common regular lattice of unit step length b and with a coordination number c, with $c = 2d$ for the hypercubic lattice in d dimensions and $c = 12$ for the $3d$ FCC lattice. While in the general case of ideal random trees, the functionality f of tree nodes (i.e., the number of other nodes they are connected to) is not restricted, below we mostly focus on the case where $f \leq 3$ so that our trees are composed of $\{N_1, N_2, N_3\}$ nodes of functionality $f = 1, 2, 3$, with $N_{\text{tree}} = N_1 + N_2 + N_3$ and the straightforward relations,

$$N_1(N_{\text{tree}}, N_3) = N_3 + 2, \tag{1}$$

$$N_2(N_{\text{tree}}, N_3) = N_{\text{tree}} - 2N_3 - 2, \tag{2}$$

between node compositions. At the end, we briefly consider the general case (treated in detail in Sec. S6 in the supplementary material).

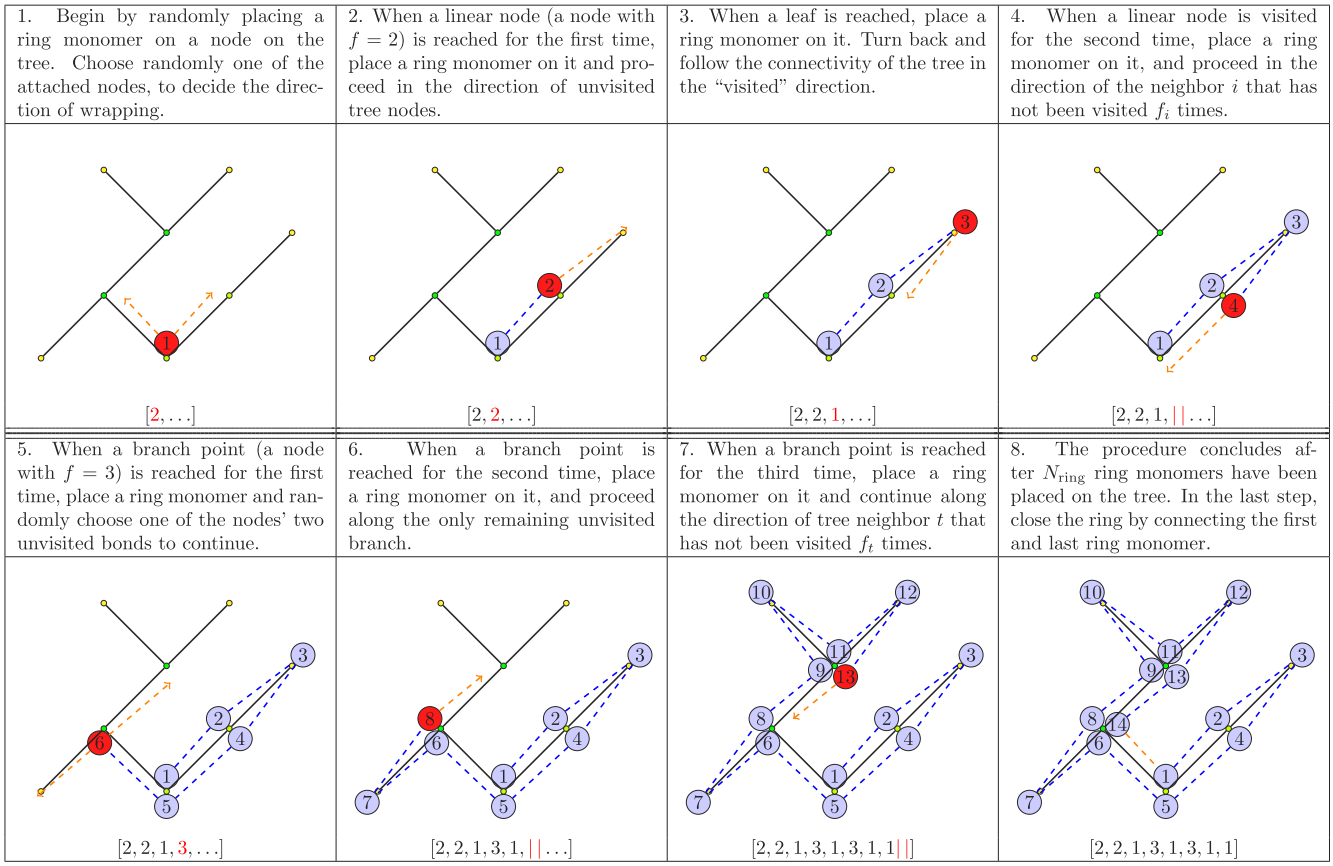

FIG. 2. Rules to construct a tightly double-folded ring polymer (violet circles) wrapped around a tree and how to translate this into a corresponding wrapping code. At each step, the last placed ring monomer is colored in red. The possible directions of the wrapping procedure are indicated by the orange arrows. In every frame, the evolving construction of the wrapping code is shown in correspondence with the placed ring monomers. When a ring monomer is placed that does not correspond to a new entry in the wrapping code, this is indicated by the symbol "‖".

WRAPPED TREES AND A WRAPPING CODE

Following the procedure originally outlined in Ref. 27 and described in detail in Fig. 2, double-folding forces the ring to traverse each tree bond twice, so a tree of size N_{tree} is wrapped by a double-folded ring of length $2(N_{\text{tree}}-1)$. In the course of the wrapping procedure, every tree node t is visited exactly f_t times. Given a tree with N_3 branch-nodes, the wrapping can be performed in

$$2(N_{\text{tree}}-1)\times 2^{N_3} \tag{3}$$

distinct ways, where the factor $2(N_{\text{tree}}-1)$ denotes the number of circular permutations of the ring (i.e., the possibility of choosing which ring monomer gets the label $i=1$) and the factor 2^{N_3} enumerates the different directions of wrapping that can be chosen when encountering a branch-node (i.e., step 5 in Fig. 2).

The wrapping code records the order in which new tree nodes are encountered along the ring. Importantly, walking along the labeled ring starting from the ring monomer $i=1$, one can encode the configuration by noting the functionalities (Fig. 2),

$$[f_1,\ldots,f_{N_{\text{tree}}}], \tag{4}$$

of newly encountered tree nodes. As illustrated in Sec. S1 in the supplementary material, a wrapping sequence contains the information to reconstruct the unique configuration of a double-folded ring polymer. In particular, any permutation in the wrapping sequence corresponds to a different set of monomer pairings or secondary structure. There is thus a one-to-one correspondence between the configuration of a double-folded ring polymer and the wrapping code. To specify the polymer's conformation, one must additionally record, during the wrapping process, each newly encountered tree-bond vector, $\{\vec{b}_1=\vec{r}_2-\vec{r}_1,\ldots,\vec{b}_{N_{\text{tree}}-1}\}$, where $\vec{r}_i$ is the spatial position of node i (with $i=1,\ldots,N_{\text{tree}}$) in the embedding space.

THE TOTAL NUMBER OF VIABLE WRAPPING CODES

Not every generic N_{tree}-long succession of 1's, 2's, and 3's corresponds to a legitimate double-folded ring. For instance, the procedure illustrated in Fig. 2 implies that a proper wrapping code must always end with $f_{N_{\text{tree}}}=1$ because the tree node with index $=N_{\text{tree}}$ is by definition only visited for the first (and hence only) time toward the end of the wrapping procedure. For given values (N_{tree},N_3), this constraint leaves

$$\frac{(N_{\text{tree}}-1)!}{(N_1-1)!\,N_2!\,N_3!} \tag{5}$$

potential orderings of the first $N_{\text{tree}}-1$ entries of a wrapping code.

The condition that the ring must only be closed with the last placed bond rules out a code like [1, 1, 3, 1], where the ring would already be closed after two steps (see Fig. S2 in the supplementary material). To see when the reading of a wrapping code leads to an error, it is useful to keep a count n_f of the numbers of f's read. The ring cannot close prematurely as long as $n_1<n_3+2$ because then the encountered trees nodes do not fulfill the condition for a wrappable sub-tree. Using the global constraint $N_1=N_3+2$, this is equivalent to the condition $N_1-n_1>N_3-n_3$ for the rest of the wrapping code.

Now, consider reading the code backwards. Then, the first entry is always a '1,' and the above condition for a viable wrapping code implies that for the remaining $N_{\text{tree}}-1$ entries, the number of 3's may never be ahead of the number of 1's. The probability for this to be the case in a random sequence of $N_1-1=N_3+1$ 1's and N_3 3's is given by a generalized form of Bertrand's "ballot theorem"[43] that permits *ties* (see Sec. S2 in supplementary material for details), namely, the fraction of valid sequences is

$$\frac{2}{N_3+2}. \tag{6}$$

Multiplying the total number of admissible permutations in Eq. (5) by the ballot-theorem fraction in Eq. (6), we obtain the total number of viable wrapping codes and thus of tightly double-folded rings configurations for given (N_{tree},N_3),

$$\Omega_{\text{ring}}(N_{\text{tree}},N_3)=\frac{2(N_{\text{tree}}-1)!}{N_1!\,N_2!\,N_3!}, \tag{7}$$

with N_1 and N_2 given by Eqs. (1) and (2), respectively.

CONTROLLING THE BRANCHING ACTIVITY

The branching activity of the double-folded rings can be controlled via a chemical potential μ_3[35,36,44,45] in the partition function for tightly double-folded rings,

$$Z_{\text{ring}}=Z_{\text{ring}}(N_{\text{tree}},\mu_3)=c^{N_{\text{tree}}-1}\sum_{N_3=0}^{N_{3,\max}}\Omega_{\text{ring}}(N_{\text{tree}},N_3)\exp(\beta\mu_3 N_3), \tag{8}$$

where $N_{3,\max}=(N_{\text{tree}}-2)/2$ for N_{tree} even and $N_{3,\max}=(N_{\text{tree}}-3)/2$ for N_{tree} odd [see Eq. (2)] and c is the coordination number of the embedding lattice.

ACCOUNTING FOR THE REPTONS IN THE ELASTIC LATTICE MODEL

The elasticity in our lattice model[28,29] of tightly double-folded rings emerges from the ring-bond length being either zero or equal to the lattice spacing [see Fig. 1(a3)]. However, up to this point, the theory was formulated at fixed tree size N_{tree}. To compare with the elastic lattice model, we now switch to an ensemble at fixed ring length N_{ring} in which the ring-bond length, and so the size N_{tree} of the underlying tree, fluctuates. Now, the probability to observe a double-folded ring conformation with N_{tree} and N_3 is given by

$$p(N_{\text{tree}},N_3|N_{\text{ring}},\mu_3)=\frac{\Omega_{\text{rep}}(N_{\text{ring}},N_{\text{tree}})\,\Omega_{\text{ring}}(N_{\text{tree}},N_3)\,e^{\beta\mu_3 N_3}}{Z_{\text{elastic}}(N_{\text{ring}},\mu_3)}, \tag{9}$$

where $\Omega_{\text{rep}}(N_{\text{ring}},N_{\text{tree}})$ is the number of ways to place zero-length bonds ("reptons") on a ring (see Sec. S3 in the supplementary material) and where

$$Z_{\text{elastic}}(N_{\text{ring}},\mu_3)=\sum_{N_{\text{tree}}}\Omega_{\text{rep}}(N_{\text{ring}},N_{\text{tree}})\,Z_{\text{ring}}(N_{\text{tree}},\mu_3) \tag{10}$$

is the partition function of the elastic system. Expectation values for the tree size and the number of $f = 1, 2, 3$-functional nodes as a function of (N_{ring}, μ_3) can be calculated by numerically summing

$$\langle N_{\text{tree}} \rangle = \sum_{N_{\text{tree}}} \sum_{N_3} N_{\text{tree}}\, p(N_{\text{tree}}, N_3 | N_{\text{ring}}, \mu_3), \tag{11}$$

$$\langle N_3 \rangle = \sum_{N_{\text{tree}}} \sum_{N_3} N_3\, p(N_{\text{tree}}, N_3 | N_{\text{ring}}, \mu_3). \tag{12}$$

The values for $\langle N_1 \rangle$ and $\langle N_2 \rangle$ follow then from Eqs. (1) and (2). For more details, see Sec. S3 in the supplementary material.

COMPARISON TO SIMULATION RESULTS

To validate our results, we have performed computer simulations of our elastic lattice model[28,29] for tightly double-folded rings, where we included the possibility into the code to control the branching activity along the lines of Eq. (8). We have generated double-folded rings polymers for lengths $N_{\text{ring}} \in [64, 216, 512, 1000]$ and chemical potentials $\beta\mu_3 \in [0, -2, -4, -6, -8]$. All simulated samples consist of 200 independent double-folded ring conformations. For details of the implementation, the equilibration procedure, and the simulations, we refer the reader to Refs. 28 and 29.

As visually represented in Fig. 3, the sampled datapoints (red dots) all fall around the peaks of the theoretical distributions, Eq. (9), into bins with expected sampling probabilities $p(N_{\text{tree}}, N_3 | N_{\text{ring}}, \mu_3) \gtrsim 10^{-2}$. A more rigorous validation, based on a statistical quantitative test, that Eq. (9) correctly represents the underlying distribution of sampled datapoints is described in detail in Sec. S4 in the supplementary material. Finally, Fig. 4 shows (main panel) the corresponding averages for $\langle N_1 + N_3 \rangle/2$ and $\langle N_2 \rangle$ normalized to $\langle N_{\text{tree}} \rangle$ as well as (inset) for $\langle N_{\text{tree}} \rangle$

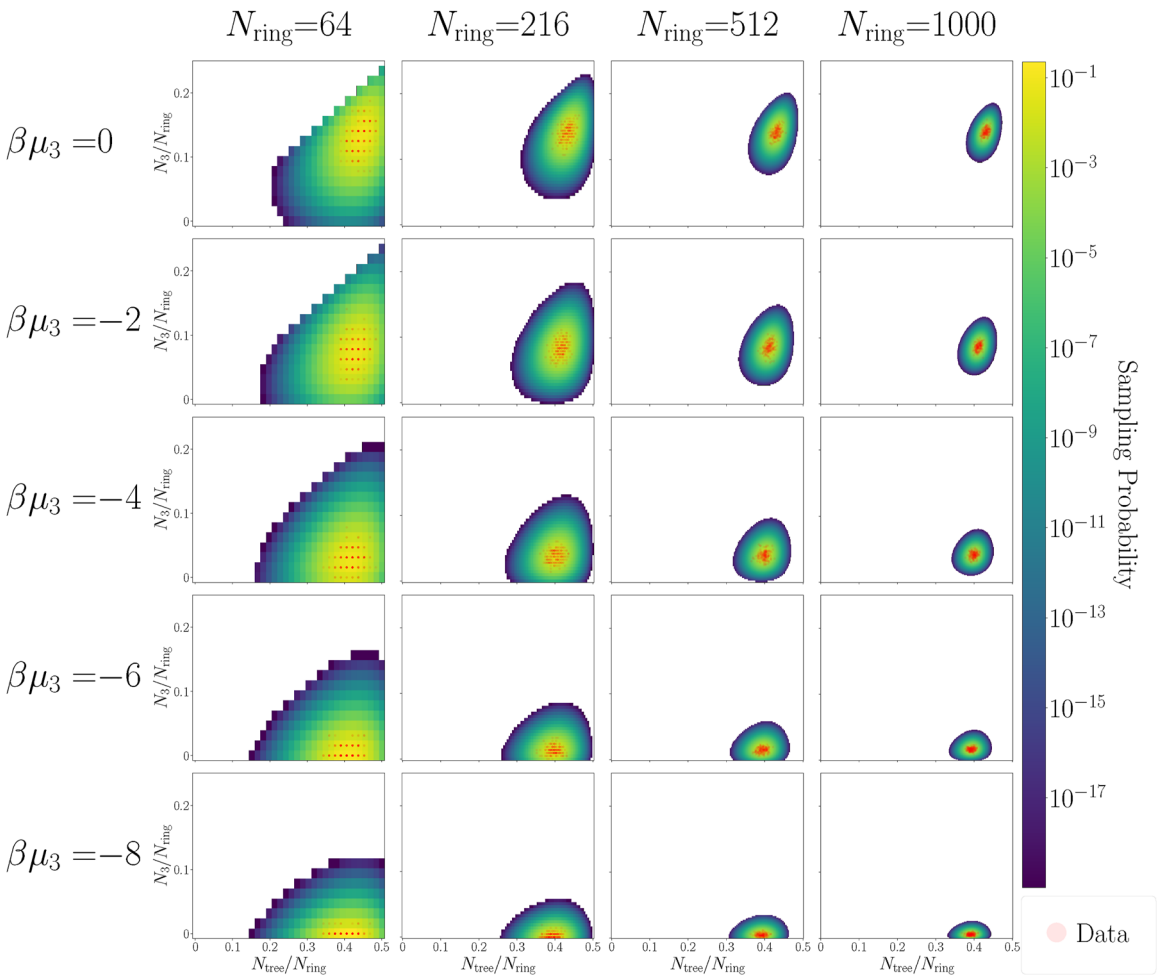

FIG. 3. Density map representation of the 2*d* probability distributions [Eq. (9)] of sampling a tuple (N_{tree}, N_3) at a given N_{ring} and for different values (see legends) of the branching chemical potential $\beta\mu_3$. Yellow/blue regions are more/less likely to be sampled, as indicated by the color bar on the right. Tuples with a probability of sampling $<10^{-19}$ are white in the above plots. The red dots represent the sampled data points from computer simulations of the elastic polymer model; they all fall on the maxima of the predicted probability distributions with no systematic deviations observed.

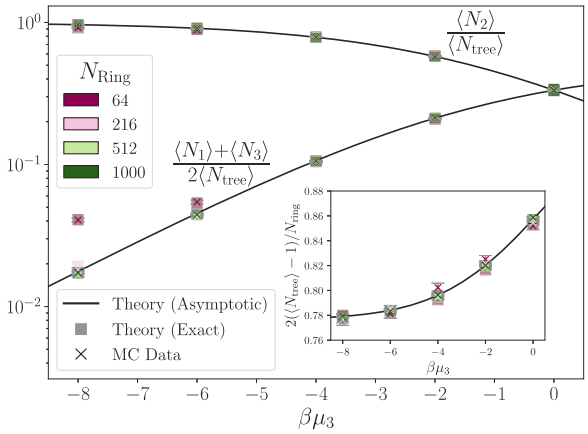

FIG. 4. Expectation values of node functionalities normalized to the mean tree size $\langle N_{\rm tree}\rangle$ (main panel) and mean tree size normalized to the ring size $N_{\rm ring}$ (inset) as a function of the branching chemical potential $\beta\mu_3$. Results: ("×"-symbols) sampled averages of the elastic lattice model; (square-symbols) numerically evaluated sums Eqs. (11) and (12); and (lines) analytical asymptotic formulas [Eqs. (15)–(17)].

− 1 normalized to $N_{\rm ring}/2$. Not surprisingly, the sampled averages ("×"-symbols) are also in good agreement with the numerically evaluated sums (square-symbols).

ANALYSIS OF THE ASYMPTOTIC BEHAVIOR

In Sec. S5 A in the supplementary material, we show that the partition function for double-folded rings, Eq. (8), is asymptotically dominated, up to power-law corrections, by the exponential term,

$$Z_{\rm ring}(N_{\rm tree},\mu_3)\sim\left(\frac{c}{1-2\lambda}\right)^{N_{\rm tree}}, \tag{13}$$

with

$$\lambda(\mu_3)=\left(2+\exp\left(-\beta\mu_3/2\right)\right)^{-1}. \tag{14}$$

Using Stirling's approximation for $\Omega_{\rm rep}(N_{\rm ring},N_{\rm tree})$ [Eq. (S6) in the supplementary material] and keeping only the dominant tree size in Eq. (10), one finds (see Sec. S5 B in the supplementary material)

$$\frac{\langle N_{\rm tree}\rangle-1}{N_{\rm ring}/2}\approx\left(\sqrt{\frac{1-2\lambda}{c}}+1\right)^{-1}, \tag{15}$$

and Eqs. (11) and (12) can be approximated as

$$\frac{\langle N_1\rangle-1}{\langle N_{\rm tree}\rangle}=\frac{\langle N_3\rangle+1}{\langle N_{\rm tree}\rangle}\approx\lambda \tag{16}$$

so that

$$\frac{\langle N_2\rangle}{\langle N_{\rm tree}\rangle}\approx 1-2\lambda. \tag{17}$$

The corresponding lines in Fig. 4 (main panel and inset) are in excellent agreement with the numerical data points for the explored values of $N_{\rm ring}$. Similarly, we have also found excellent agreement between the predicted distribution of reptons on nodes of given functionality [which is described by a beta-binomial law, see Eq. (S25) in the supplementary material] and the numerical data (for an in-depth discussion, see Sec. S5 C in the supplementary material).

ARBITRARY NODE FUNCTIONALITIES

In general, a ring wrapping a tree passes each tree node t exactly f_t times. This implies that the wrapping procedure has $(f_t-1)!$ choices of direction for wrapping per tree node t. Reversing the arguments for Eq. (7) and Sec. S1 in the supplementary material, by assigning to each labeled[46] tree a multiplicity of $(f_t-1)!$ per tree node of functionality f_t, we *conjecture* that the generalized version of Eq. (7) is given by

$$\Omega_{\rm ring}(N_{\rm tree},\{N_f\})=2\frac{(N_{\rm tree}-1)!}{N_1!\ldots N_{f_{\rm max}}!}, \tag{18}$$

where $f_{\rm max}$ is nodes' maximal functionality. From Eq. (18), all previously derived results can be extended accordingly. In Sec. S6 in the supplementary material, we derive a polynomial identity, Eq. (S36) in the supplementary material, that needs to be solved numerically to approximate the expected number of tree-nodes $\langle N_f\rangle$, for given functionality f and corresponding set of branching chemical potentials $\{\mu_1,\ldots,\mu_{f_{\rm max}}\}$. Notably, there are two simple limiting cases for chemical potentials $\{\mu_f=0\}$,

$$\lim_{N_{\rm tree}\to\infty}\frac{\langle N_f\rangle}{N_{\rm tree}}=\begin{cases}1/3 & \text{if } f_{\rm max}=3,\\ 2^{-f} & \text{if } f_{\rm max}=\infty.\end{cases} \tag{19}$$

In Fig. 5, we show that data from the supporting information of Ref. 29 for $N_{\rm ring}=216$, $\{\mu_f=0\}$ and maximal functionalities up to $f_{\rm max}=12$ (symbols) are in good agreement with the theoretical expressions (lines). The (essentially) equal prevalence of $f=1,2,3$ functional nodes for $f_{\rm max}=3$ corresponds to the crossing of the lines in the main panel of Fig. 4, while the functionality distributions for $f_{\rm max}>3$ quickly approach the asymptotic 2^{-f} behavior.

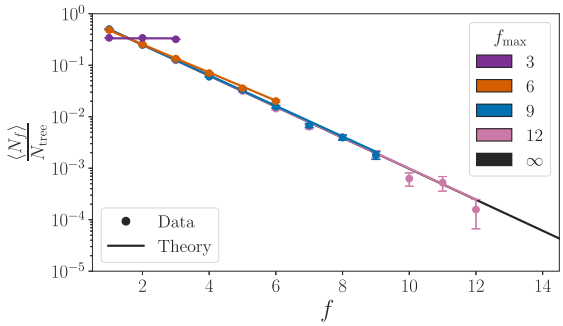

FIG. 5. Mean number of nodes of functionality f for trees with maximal nodes' functionality $f_{\rm max}$ and branching chemical potentials $\{\mu_f=0\}$. Symbols and lines are for sampled averages of the elastic lattice model and our theory.

CONCLUSION AND OUTLOOK

To summarize, we have introduced a wrapping code for characterizing the secondary structure of double-folded rings, which allowed us to count the number of available configurations for freely jointed rings in the absence of volume interactions. Resulting predictions for ensembles with controlled branching activity are in excellent agreement with data from Monte Carlo simulations of an elastic lattice model of non-interacting tightly double-folded rings. In a forthcoming publication,[47] we will establish a coherent framework for the modeling of double-folded rings on the ring and on the tree level, which is based on a direct mapping between the two ensembles explored here and in Ref. 46. Importantly, this connection enables to leverage the computational efficiency of MC algorithms for randomly branched polymers[45] in ring studies, including volume interactions like excluded-volume effects, which are, of course, relevant in realistic systems. Ultimately, we aim at studying the consequences of topological constraints on the organization of entire genomes.[48]

SUPPLEMENTARY MATERIAL

The supplementary material contains a section illustrating the decoding of the wrapping code, a presentation with demonstration of the "ballot theorem," the derivation of the statistical weight of reptons, a validation of Eq. (9) using a statistical test, formulas for the trees/rings asymptotic behavior, treatment of trees with nodes of arbitrary functionality, and additional figures.

ACKNOWLEDGMENTS

P.H.W.v.d.H. acknowledges financial support from Grant No. PNRR_M4C2I4.1._DM351 funded by NextGenerationEU and the kind hospitality of the ENS-Lyon. A.R. acknowledges financial support from PNRR Grant Nos. CN_00000013_CN-HPC and M4C2I1.4, spoke 7, funded by Next Generation EU. E.G. acknowledges computing time of the CBPSmn computer cluster of the ENS-Lyon where simulations were performed.

AUTHOR DECLARATIONS

Conflict of Interest

The authors have no conflicts to disclose.

Author Contributions

Pieter H. W. van der Hoek: Conceptualization (supporting); Data curation (equal); Formal analysis (lead); Investigation (lead); Methodology (equal); Software (supporting); Validation (equal); Visualization (lead); Writing – original draft (lead); Writing – review & editing (supporting). **Angelo Rosa**: Conceptualization (equal); Investigation (equal); Methodology (equal); Supervision (equal); Validation (equal); Writing – original draft (supporting); Writing – review & editing (supporting). **Elham Ghobadpour**: Data curation (equal); Investigation (supporting); Software (lead); Validation (supporting). **Ralf Everaers**: Conceptualization (equal); Investigation (equal); Methodology (equal); Supervision (equal); Validation (equal); Writing – review & editing (lead).

DATA AVAILABILITY

The data that support the findings of this study are available from the corresponding author upon reasonable request. The simulation software is an open-source package, distributed under the GNU General Public License v3.0 and written in C++, it is available at https://doi.org/10.5281/zenodo.14893438.

REFERENCES

[1] J. F. Marko and E. D. Siggia, Science **265**, 506 (1994).
[2] J. F. Marko and E. D. Siggia, Phys. Rev. E **52**, 2912 (1995).
[3] C. L. Woldringh and T. Odijk, "Structure of DNA within the bacterial cell: Physics and physiology," in *Organization of the Prokaryotic Genome* (Wiley, 1999), pp. 171–187.
[4] S. Cunha, C. L. Woldringh, and T. Odijk, J. Struct. Biol. **136**, 53 (2001).
[5] E. Alipour and J. F. Marko, Nucleic Acids Res. **40**, 11202 (2012).
[6] A. L. Sanborn, S. S. P. Rao, S.-C. Huang, N. C. Durand, M. H. Huntley, A. I. Jewett, I. D. Bochkov, D. Chinnappan, A. Cutkosky, J. Li, K. P. Geeting, A. Gnirke, A. Melnikov, D. McKenna, E. K. Stamenova, E. S. Lander, and E. L. Aiden, Proc. Natl. Acad. Sci. U. S. A. **112**, E6456 (2015).
[7] G. Fudenberg, M. Imakaev, C. Lu, A. Goloborodko, N. Abdennur, and L. A. Mirny, Cell Rep. **15**, 2038 (2016).
[8] A. Goloborodko, J. F. Marko, and L. A. Mirny, Biophys. J. **110**, 2162 (2016).
[9] A. Goloborodko, M. V. Imakaev, J. F. Marko, and L. Mirny, eLife **5**, e14864 (2016).
[10] A. Grosberg, Y. Rabin, S. Havlin, and A. Neer, Europhys. Lett. **23**, 373 (1993).
[11] T. Cremer and C. Cremer, Nat. Rev. Genet. **2**, 292 (2001).
[12] A. Rosa and R. Everaers, PLoS Comput. Biol. **4**, e1000153 (2008).
[13] E. Lieberman-Aiden, L. van Berkum Nynke, L. Williams, M. Imakaev, T. Ragoczy, A. Telling, I. Amit, B. R. Lajoie, P. J. Sabo, M. O. Dorschner, R. Sandstrom, B. Bernstein, M. A. Bender, M. Groudine, A. Gnirke, J. Stamatoyannopoulos, L. A. Mirny, E. S. Lander, and J. Dekker, Science **326**, 289 (2009).
[14] A. Rosa, N. B. Becker, and R. Everaers, Biophys. J. **98**, 2410 (2010).
[15] A. R. Khokhlov and S. K. Nechaev, Phys. Lett. A **112**, 156 (1985).
[16] M. Rubinstein, Phys. Rev. Lett. **57**, 3023 (1986).
[17] S. P. Obukhov, M. Rubinstein, and T. Duke, Phys. Rev. Lett. **73**, 1263 (1994).
[18] A. Y. Grosberg, Soft Matter **10**, 560 (2014).
[19] J. Smrek and A. Y. Grosberg, J. Phys.: Condens. Matter **27**, 064117 (2015).
[20] J. D. Halverson, W. B. Lee, G. S. Grest, A. Y. Grosberg, and K. Kremer, J. Chem. Phys. **134**, 204904 (2011).
[21] D. Michieletto, Soft Matter **12**, 9485 (2016).
[22] A. Rosa and R. Everaers, Phys. Rev. Lett. **112**, 118302 (2014).
[23] R. D. Schram, A. Rosa, and R. Everaers, Soft Matter **15**, 2418 (2019).
[24] J. Smrek, K. Kremer, and A. Rosa, ACS Macro Lett. **8**, 155 (2019).
[25] M. A. Ubertini and A. Rosa, Soft Matter **21**, 8711 (2025).
[26] C. M. Schroeder, R. Everaers, K. Kremer, M. Kruteva, C. N. Likos, G. B. McKenna, T. O'Connor, J. Ravi Prakash, D. Richter, R. Robertson-Anderson, M. Rubinstein, K. S. Schweizer, and D. Vlassopoulos, J. Rheol. **70**, 183 (2026).
[27] A. Rosa and R. Everaers, Eur. Phys. J. E **42**, 7 (2019).
[28] E. Ghobadpour, M. Kolb, M. R. Ejtehadi, and R. Everaers, Phys. Rev. E **104**, 014501 (2021).
[29] E. Ghobadpour, M. Kolb, I. Junier, and R. Everaers, Macromolecules **58**, 10632 (2025).
[30] M. Rubinstein, Phys. Rev. Lett. **59**, 1946 (1987).

[31] M. Doi and S. F. Edwards, *The Theory of Polymer Dynamics* (Oxford University Press, New York, 1986).
[32] M. Rubinstein and R. H. Colby, *Polymer Physics* (Oxford University Press, New York, 2003).
[33] E. J. J. v. Rensburg and N. Madras, J. Phys. A: Math. Gen. **25**, 303 (1992).
[34] H.-P. Hsu, W. Nadler, and P. Grassberger, J. Phys. A: Math. Gen. **38**, 775 (2005).
[35] A. Rosa and R. Everaers, J. Phys. A: Math. Theor. **49**, 345001 (2016).
[36] A. Rosa and R. Everaers, J. Chem. Phys. **145**, 164906 (2016).
[37] S. M. Bhattacharjee, A. Giacometti, and A. Maritan, J. Phys.: Condens. Matter **25**, 503101 (2013).
[38] R. Everaers, A. Y. Grosberg, M. Rubinstein, and A. Rosa, Soft Matter **13**, 1223 (2017).
[39] T. C. Lubensky and J. Isaacson, Phys. Rev. A **20**, 2130 (1979).
[40] G. Parisi and N. Sourlas, Phys. Rev. Lett. **46**, 871 (1981).
[41] P. D. Gujrati, Phys. Rev. Lett. **74**, 809 (1995).
[42] H.-K. Janssen and O. Stenull, Phys. Rev. E **83**, 051126 (2011).
[43] J. Bertrand, C. R. Acad. Sci. Paris **105**, 369 (1887).
[44] A. Rosa and R. Everaers, Phys. Rev. E **95**, 012117 (2017).
[45] P. H. W. van der Hoek, A. Rosa, and R. Everaers, Phys. Rev. E **110**, 045312 (2024).
[46] P. H. W. van der Hoek, A. Rosa, and R. Everaers, Phys. Rev. E **112**, 065405 (2025).
[47] P. H. W. van der Hoek, A. Rosa, E. Ghobadpour, and R. Everaers, "Coherent modeling of double-folded ring polymers and their underlying random tree structure" (unpublished).
[48] E. Ghobadpour, "Multiple scale modeling of bacterial chromosome," Ph.D. thesis, Université Grenoble Alpes, 2023.